Accelerated Publications

Conformation of a Cdc42/Rac Interactive Binding Peptide in Complex with Cdc42 and Analysis of the Binding Interface†

Willem K. Stevens, Wim Vranken, Nathalie Goudreau, Hui Xiang, Ping Xu, and Feng Ni*

Biomolecular NMR Laboratory and Montreal Joint Centre for Structural Biology, Biotechnology Research Institute, National Research Council of Canada, 6100 Royalmount Avenue, Montreal, Quebec, H4P 2R2 Canada

Received February 23, 1999; Revised Manuscript Received April 2, 1999

ABSTRACT: Most of the putative effectors for the Rho-family small GTPases Cdc42 and Rac share a common sequence motif referred to as the Cdc42/Rac interactive binding (CRIB) motif. This sequence, with a consensus of I-S-x-P-$(x)_{2-4}$-F-x-H-x-x-H-V-G [Burbelo, P. D., et al. (1995) *J. Biol. Chem. 270*, 29071−29074], has been shown to be essential for the functional interactions between these effector proteins and Cdc42. We have characterized the interactions of a 22-residue CRIB peptide derived from human PAK2 [PAK2(71−92)] with Cdc42 using proton and heteronuclear NMR spectroscopy. This CRIB peptide binds to GTP-γS-loaded Cdc42 in a saturable manner, with an apparent K_d of 0.6 μM, as determined by fluorescence titration using sNBD-labeled Cdc42. Interaction of the 22-residue peptide PAK2(71−92) with GTP-γS-loaded Cdc42 causes resonance perturbations in the $^1H-^{15}N$ HSQC spectrum of Cdc42 that are similar to those observed for a longer (46-amino acid) CRIB-containing protein fragment [Guo, W., et al. (1998) *Biochemistry 37*, 14030−14037]. Proton NMR studies of PAK2(71−92) demonstrate structuring of PAK2(71−92) in the presence of GTP-γS-loaded Cdc42, through the observation of many nonsequential transferred NOEs. Structure calculations based on the observed transferred NOEs show that the central portion of the Cdc42-bound CRIB peptide assumes a loop conformation in which the side chains of consensus residues Phe80, His82, Ile84, His85, and Val86 are brought into proximity. The CRIB motif may therefore represent a minimal interfacial region in the complexes between Cdc42 and its effector proteins.

The Rho-like GTPases Cdc42 and Rac are important components of the cell signal-transduction machinery and play roles in transcriptional activation (*1*−*3*), cytoskeletal organization, and shape change (*4*, *5*). Activities of Cdc42 and Rac are also implicated in diverse physiological and pathological processes, including human cognitive function (*6*), apoptosis (*7*), and development of an invasive phenotype (*8*) for some cell lines. Functions of Cdc42 and Rac are mediated through representatives of a growing family of candidate effectors (*9*), including the p21-activated serine/threonine protein kinases (PAKs)[1] (*10*), Cdc42-associated tyrosine kinases ACK-1 and ACK-2 (*11*, *12*), the myotonic dystrophy-related Cdc42-binding kinases (*13*), the non-kinase, Wiscott-Aldrich syndrome protein (*14*), the 70 kDa S6 kinase (*2*), and the IQGAPs (*15*). Except for the S6 kinase and IQGAPs, these putative effector proteins share a consensus sequence of I-S-x-P-$(x)_{2-4}$-F-x-H-x-x-H-V-G, known as the Cdc42/Rac interactive binding (CRIB) motif (*9*, *16*, *17*). This sequence motif appears in at least 25 distinct proteins from a variety of organisms. The CRIB region has been shown to be essential for mediating interactions between Cdc42 and its effector proteins, through truncation studies of the PAK1 and WASP proteins (*9*, *14*).

The best characterized CRIB-containing Cdc42 effectors are the PAK family of protein kinases, and their yeast homologues Ste20 and Cla4. In *Saccharomyces cerevisiae*, Ste20 interacts with Cdc42 and several other components of the mating signal pathway, leading to activation of the pheromone-response MAP kinase pathways. The interaction between Ste20 and Cdc42 mediated by the CRIB sequence is necessary for filamentous growth upon nitrogen starvation, and for an undefined essential function shared with Cla4 (*18*). The Cdc42−CRIB interaction also localizes Ste20 to areas of polarized cell growth (*18*). Studies of mammalian PAKs indicate that the CRIB-mediated interaction with Cdc42 or Rac has functional consequences for both binding partners. Cdc42 binding leads to PAK activation for PAKs 1−3 (*10*, *11*) and localization of PAK4 to the Golgi (*19*). At the same

† This work was supported by the National Research Council of Canada (NRCC publication 42908).

* Corresponding author.

[1] Abbreviations: ACK, Cdc42-associated protein kinase; PAK, p21-associated protein kinase; MAP kinase, mitogen-activated protein kinase; MRCK, myotonic dystrophy-related protein kinase; WASP, Wiscott-Aldrich syndrome protein; GST, glutatione *S*-transferase; NOE, nuclear Overhauser effect; NOESY, nuclear Overhauser effect spectroscopy; TOCSY, total correlation spectroscopy; HSQC, heteronuclear single-quantum coherence spectroscopy; PMSF, phenylmethanesulfonyl fluoride; GTP-γS, guanosine 5′-*O*-(thiotriphosphate); GMPPCP, β,γ-methylene derivative of GTP; sNBD, succinimidyl 6-[(7-nitrobenz-2-oxa-1,3-diazol-4-yl)amino]hexanoate; PPACk, D-Phe-Pro-Arg-chloromethyl ketone.

10.1021/bi990426u CCC: $18.00 Published 1999 by the American Chemical Society
Published on Web 04/20/1999

time, CRIB-dependent effector binding decreases the GTPase activity and the rate of nucleotide dissociation from Cdc42 (*21*).

The exact determinants for the CRIB−Cdc42 interaction are not yet clear. It is generally accepted that the consensus CRIB sequence is essential for binding, but a number of studies suggest that further sequences are required for maintaining high-affinity interactions (*20*, *21*, *25)*. Recently, detailed biochemical studies of extended binding sequences from human PAK1(51−135), mPAK3(65−137), and WASP have revealed high-affinity, solution-phase binding between these protein fragments and Cdc42 (*21*−*23*). NMR studies of the interaction between Cdc42 and a 46-residue CRIB-containing protein fragment from mPAK3 identified an extended binding interface on the surface of Cdc42, with conformational rearrangements of Cdc42 accompanying binding (*24*). Additional data indicate that conserved residues C-terminal to the CRIB motif are involved in negative regulation of the catalytic activities of the PAK kinases, and that the 60 residues of PAK preceding the CRIB region make little contribution to binding (*25*). Therefore, sequences outside the CRIB region appear to have alternative functions in addition to bolstering binding between the CRIB motif and Cdc42.

In this study, we determine the conformation of a CRIB motif ligand bound to Cdc42 and characterize its binding interactions. Proton NMR spectroscopy was used to probe for structuring of the CRIB peptide PAK2(71−92), derived from human PAK2 in the presence of the "inactive" (GDP-loaded) or "active" (GTP-γS-loaded) form of Cdc42. Heteronuclear NMR spectroscopy was used to map the regions on the surface of Cdc42 involved in interactions with this CRIB peptide. We also attempt to address the role of the CRIB motif in the formation of selective and high-affinity complexes between Cdc42 and the CRIB-containing protein effectors.

MATERIALS AND METHODS

Peptide Synthesis and Purification. Peptides corresponding to residues 71−92 and residues 69−117 of human PAK2 (Genbank accession number S58682) were synthesized using standard FMOC chemistry at the Sheldon Biotechnology Service Center of McGill University (Montreal, PQ). The peptides were purified by reversed-phase HPLC and their identities verified by electrospray mass spectrometry. Samples for NMR experiments were prepared by dissolving 1−2 mg of the lyophilized peptide in 450 μL of an aqueous buffer composed of 50 mM sodium phosphate, 50 mM sodium chloride, and 2 mM magnesium chloride at pH 6.8 with 1 mM sodium azide added as a preservative. The deuterium lock signal for the NMR spectrometers was provided by the addition of 50 μL of D_2O.

Protein Purification. A plasmid encoding recombinant human Cdc42 as a glutathione *S*-transferase fusion protein was generously supplied by G. M. Bokoch. This construct was used in *Escherichia coli* strain BL21(DE3) to express GST−Cdc42 which was subsequently purified on glutathione Sepharose (Pharmacia) essentially as previously described (*26*). For heteronuclear NMR experiments, Cdc42 was uniformly labeled with the ^{15}N and ^{13}C isotopes using ^{15}N- and ^{13}C-enriched Bio-Express-1000 cell growth medium (Cambridge Isotope Laboratories, Andover, MA). Immediately prior to use, Cdc42 was nucleotide exchanged to the GTP-γS-bound form. Briefly, GTP-γS was added at a 10-fold excess in the presence of 6.7 mM EDTA. After the exchange reaction was allowed to take place (10 min), the reaction was stopped with the addition of $MgCl_2$ to a 2 mM excess over the EDTA that was present. The sample was then buffer exchanged by centrifugal ultrafiltration to remove excess EDTA and nucleotide, and concentrated to 1 mM prior to NMR titration experiments.

Fluorescence Titration. For fluorescence binding studies, Cdc42 was labeled with succidinimidyl 6-[(7-nitrobenz-2-oxa-1,3-diazol-4-yl)amino]hexanoate (sNBD) prior to elution from the glutathione Sepharose column as described by Nomanbhoy et al. (*27*). Interaction of the CRIB peptides with sNBD-labeled Cdc42 was monitored using extrinsic fluorescence measurements with a Perkin-Elmer MPF-66 fluorescence spectrophotometer. Samples of GTP-γS-loaded and sNBD-labeled Cdc42 were added in the indicated buffers to a cuvette being continuously stirred. The sample was excited at 488 nm with an excitation slit width of 5 nm. The emission intensity was monitored continuously at 545 nm with a 530 nm band-pass filter in place, as aliquots of the peptide were added from a concentrated (1 mM) stock.

Proton NMR Experiments. Proton NMR experiments were carried out on Bruker AMX2/Avance-500 or Avance-800 spectrometers. Sample temperatures were 25 or 30 °C. Phase sensitive detection by time-proportional phase incrementation was employed for both two-dimensional Overhauser effect NOESY (*28*) and total correlation TOCSY (*29*, *30*) experiments. Mixing times of 150 and 200 ms were used for NOESY experiments, and a mixing time of 65 ms was used for TOCSY experiments. Spectral processing was carried out using the XwinNMR software package (Bruker). Spectral display, analysis, and comparison were performed using the graphics interface of the Sybyl NMR module, TRIAD (Tripos). Transferred NOE experiments were carried out with PAK2(71−92) concentrations of 1−1.5 mM with molar ratios of peptide to GST−Cdc42 of 7.5:1 to 10:1. The peptide−protein complexes were initially characterized with NMR experiments at 500 MHz, while NOESY data collected at 800 MHz, with increased resonance dispersion and signal-to-noise, were used to obtain NOE distance constraints. In some cases, additional NMR spectra collected at 500 MHz at lower temperatures were used to resolve some overlapped resonances.

Heteronuclear Two-Dimensional and Three-Dimensional NMR Experiments. Heteronuclear NMR experiments were carried out on a Bruker Avance-800 spectrometer equipped with a 5 mm triple-resonance (^1H, ^{13}C, and ^{15}N) three-axis gradient probe using four RF channels. Equivalent sets of heteronuclear two-dimensional and three-dimensional data comprised of $^1H-^{15}N$ HSQC (*31*), HNCA (*32*), HN(CO)-CA (*33*), and CT-HNCO (*34*) spectra were collected for GTP-γS-loaded Cdc42 in the presence and absence of PAK2-(71−92). Water suppression was achieved using the WATERGATE method (*35*) with a 3:9:19 binomial selective pulse (*36*) incorporated into the last 2*t* periods in all the three-dimensional pulse sequences as described previously (*37*). To improve the sensitivity and water suppression, water magnetization was re-aligned to the $+Z$-axis before acquisition by setting the phase of the last 90° ^1H pulse to $-X$. For

Table 1: Proton Resonance Assignments (in Parts per Million) of the PAK2(71−92) Peptide[a]

residue	NH	αCH	βCH	others
Arg71		4.25	1.86	γCH_2 1.63; δCH_2 3.17
Pro72	−	4.43	1.94, 2.25	γCH_2 1.84; δCH_2 3.55, 3.68
Glu73	8.52	4.22	1.96, 2.05	γCH_2 2.22
Ile74	8.08	4.16	1.77	γCH_2 1.38; γCH_3 and δCH_3 0.82
Ser75	8.33	4.68	3.68, 3.80	
Pro76	−	4.63	1.95, 2.25	γCH_2 1.83; δCH_2 3.62, 3.76
Pro77	−	4.37	1.95, 2.25	γCH_2 1.84; δCH_2 3.54, 3.74
Ser78	8.30	4.32	3.71, 3.78	
Asp79	8.21	4.50	2.50, 2.55	
Phe80	8.02	4.47	2.95, 3.05	2,6H 7.14; 3,5H 7.26; 4H 7.22
Glu81	8.17	4.08	2.05, 2.05	γCH_2 1.81
His82	8.14	4.62	3.04, 3.17	2H 8.12; 4H 7.09
Thr83	7.97	4.20	4.04	γCH_3 1.30
Ile84	8.00	4.04	1.71	γCH_2 1.04, 1.29; γCH_3 and δCH_3 0.74
His85	8.38	4.65	2.98, 3.06	2H 8.05; 4H 7.02
Val86	8.07	4.03	1.95	γCH_3 0.82
Gly87	8.31	3.78, 3.86		
Phe88	8.04	4.56	2.91, 3.10	2,6H 7.17; 3,5H 7.27; 4H 7.22
Asp89	8.25	4.49	2.49, 2.55	
Ala90	7.95	4.26	1.29	
Val91	8.04	4.11	2.05	γCH_3 0.87
Thr92	7.70	4.11		γCH_3 1.08

[a] NMR spectra were collected at 298 K and pH 6.8 in the presence of a 1:10 molar ratio of GST−Cdc42 to peptide.

the HNCA experiment, SEDUCE-1 (*38*) decoupling with a field of 2.5 kHz was used to decouple $^{13}CO-^{15}N$ interactions in the t_1 and t_2 evolution periods. All data sets were processed using NMRPipe (*39*) with 90°-shifted sine-square weighting functions in all three dimensions. Spectral display and assignment were carried out using the XEASY software package (*40*).

Proton and Heteronuclear Backbone Resonance Assignments. Sequence-specific assignments of the proton resonances for PAK2(71−92) were achieved by combining identification of spin systems from the TOCSY spectra with sequential NOE connectivities from the NOESY spectra. All the chemical shift values (Table 1) were determined from the two-dimensional spectra and are reported with respect to an external DSS reference signal set to 0 ppm. GTP-γS-loaded Cdc42, under the conditions used in this study, yielded $^1H-^{15}N$ HSQC spectra similar to those of GMPPCP-loaded Cdc42, whose backbone ^1H, ^{13}C, and ^{15}N resonances have been assigned and reported previously (*41*). Most of the resonance assignments for GMPPCP-loaded Cdc42 at pH 5.5 could therefore be transferred to GTP-γ-S-loaded Cdc42 at pH 6.8 using three triple-resonance experiments, namely, HNCO, HNCA, and HN(CO)CA. This process provided backbone assignments for all residues except for several in the P-loop (14 and 16−20), switch I (37−41), and switch II (56−60, 62, and 64−68) regions. The absence of these signals is likely due to conformational heterogeneity and exchange in these loop regions as previously observed (*24*, *41*) and does not impede interpretation of the binding studies with the CRIB peptide. Perturbations of resonances in the HSQC spectra of GTP-γ-S-loaded Cdc42 were followed through titration of varying amounts of the PAK2(71−92) peptide. Assignments of these resonances were verified through comparison with cross-peaks in the HNCO, HNCA, and HN(CO)CA spectra of Cdc42 in the presence of the CRIB peptide.

Structure Calculations. The NOE cross-peaks of PAK2(71−92) in the presence of GST−Cdc42 were classified into groups identified as strong, medium, or weak on the basis of peak integration, with upper bounds for the corresponding interproton distances of 2.5, 3.3, and 5.0 Å, respectively. For initial structure calculations, we employed a uniform upper bound of 5 Å regardless of NOE intensities to generate a set of starting conformations that sampled a wide range of conformational space. The more restrictive distance upper bounds were used if the set of initial conformations failed to reproduce the experimental NOEs using an ensemble relaxation matrix calculation of predicted NOE intensities (*42*, *46*). Lower bounds of 3−4 Å were added for consistently predicted proximate proton pairs that do not have experimentally observed NOEs (*43*). Theoretical NOEs were calculated using peptide and Cdc42 concentrations of 1.5 and 0.2 mM, respectively, with an upper limit estimate of 0.01 mM for the dissociation constant of the Cdc42−peptide complex. The correlation times for the free peptide, the Cdc42−peptide complex, and the methyl groups were taken to be 300, 20 000, and 25 ps, respectively. The correlation time for the peptide−Cdc42 complex is a calculated estimate for a roughly spherical 50 kDa molecule in aqueous solution at 303 K; that for the free peptide was based on the close to null NOEs observed for the free peptide, and the value of 25 ps is a generally valid value for the rotation of methyl groups (*46*). Peptide conformations were generated with distance geometry calculations in which the ECEPP/3 database was employed (*44*). Minimization of the distance target function was carried out through the variable target function procedure (*45*, *46)*, by varying all the dihedral angles, except for the ω angles regulating the planarity of the peptide bond.

RESULTS

Assessment of Peptide Binding by Fluorescence Titration. The peptide derived from residues 71−92 of human PAK2 (RPEISPPSDFEHTIHVGFDAVT) chosen for our studies corresponds to the region of greatest homology between the PAK family of kinases and other Cdc42/Rac ligands (*17*), and contains the described consensus sequence I-S-x-P-$(x)_{2-4}$-F-x-H-x-x-H-V-G for the CRIB motif (*9*). Interaction of PAK2(71−92) with sNBD-labeled Cdc42 (*21*) was followed by changes in extrinsic fluorescence with the addition of varying amounts of the peptide (0−2.5 μM). Saturable and reversible binding with an apparent K_d of 0.6 μM at pH 6.8 was observed as shown in a representative titration (Figure 1). In comparison**,** a longer peptide comprising residues 69−117 of PAK2 bound to sNBD−Cdc42 with a K_d of 50 nM, similar to that observed for a 46-residue peptide of mPAK3 (*24*). In either case, the observed change in fluorescence could be reversed with the addition of excess unlabeled Cdc42. PAK2(71−92) could also be competed off sNBD−Cdc42 by addition of the longer peptide. Equivalent binding was observed in either Tris (pH 8.0) or phosphate (pH 6.8) buffer, and the latter was chosen for the subsequent NMR binding experiments.

Identification of Residues on Cdc42 Perturbed by PAK2-(71−92). Binding between PAK2(71−92) and Cdc42 was monitored by collecting $^1H-^{15}N$ HSQC spectra of GTP-γS-loaded Cdc42 in the presence of varying concentrations of the peptide. Comparison of the HSQC spectra in the presence

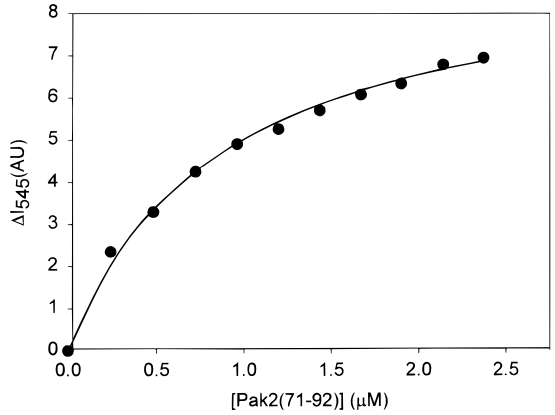

FIGURE 1: Fluorescence titration of sNBD-labeled Cdc42 with PAK2(71−92). GTP-γS-loaded Cdc42 (1 μM) in 50 mM sodium phosphate, 50 mM NaCl, and 2 mM Mg^{2+} at pH 6.8 was titrated with PAK2(71−92) while the sNBD fluorescence was monitored as described in Materials and Methods. The increment in fluorescence is plotted, and the line represents a fit of the data to a simple model for bimolecular association.

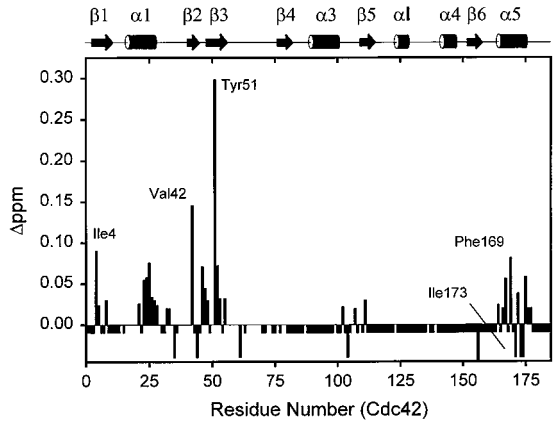

FIGURE 2: Summary of resonance perturbations in the $^1H-^{15}N$ HSQC spectra of GTP-γS-loaded Cdc42 induced by the binding of PAK2(71−92). Shifts (Δppm) are reported as a weighted vector sum of the ^1H and ^{15}N chemical shift deviations. Residues that either broadened or disappeared in the presence of PAK2(71−92) and residues that did not perceptibly shift are denoted by long and short bars below the zero line, respectively. Proline residues and residues for which assignments were not possible are left as blanks. Shown at the top of the figure is a schematic of the secondary structure elements of Cdc42 (*41*). Residues that are potential points of hydrophobic contact with the bound CRIB peptide are labeled.

and absence of PAK2(71−92) reveals a set of resonances that are either shifted or broadened in the presence of PAK2-(71−92) (Figure 2). Widespread line broadening was also observed in the amide proton resonances of the PAK2(71−92) peptide during the titration with Cdc42 or GST−Cdc42 (data not shown). These line broadening effects and chemical shift changes are indicative of a relatively fast exchange on the NMR time scale, and an averaging between the free and bound resonances (*46*). While some ambiguity is present in the regions of missing resonance assignments (see Materials and Methods), widespread resonance perturbations are observed for the N-terminal third of Cdc42. These perturbations map to the α1 helix, carrying on to the switch I region (residues 21−33), and the β2 and β3 strands (residues 42−55) flanking the switch II region, as well as the C-terminal α5 helix (residues 164−177). This pattern of resonance perturbations is qualitatively similar to that observed for the interaction of a 46-amino acid peptide in slow exchange with GMPPCP-loaded Cdc42 (*24*), suggesting a common mode and consequence of binding. However, since the complex between PAK2(71−92) and Cdc42 is in fast exchange on the NMR time scale, transferred NOE methods can be used to determine the conformation of the CRIB peptide in complex with Cdc42.

Transferred NOEs with PAK2(71−92) in the Presence of GTP-γS-Loaded Cdc42. The NOESY spectra of PAK2(71−92) in the absence of Cdc42 showed only a few sequential and intraresidue NOEs (Figure 3A). With the addition of Cdc42, the NOESY spectra revealed a group of nonsequential NOE peaks that can be transferred NOEs representative of the conformation of the Cdc42-bound peptide. Interpretation of the observed NOEs was complicated by the presence of NOE peaks from Cdc42 even with low molar ratios of protein to peptide (1:10). To reduce the NOE signals from Cdc42, subsequent NMR experiments were carried out using the full-length GST−Cdc42 fusion protein. The full-length fusion protein, with a molecular mass of ∼50 kDa, is expected to have exceedingly broad signals, satisfying the normal conditions for transferred NOE experiments (*46*). The same set of nonsequential NOEs was observed in experiments with both Cdc42 and the intact fusion proteins loaded with GTP-γS (Figure 3B), indicating that they arise solely from interactions of the peptide with the Cdc42 moiety of the fusion protein. Additional experiments carried out using GDP-loaded GST−Cdc42 (Figure 3C) showed attenuation or disappearance of many of the nonsequential NOEs observed with GTP-γS-loaded Cdc42, consistent with the reduced affinity CRIB motif peptides display for the GDP-bound form of Cdc42 (*20*, *21*). The absence of many of the long-range transferred NOEs with the GDP-bound form of Cdc42 also suggests that there may be a change in the mode of interaction between CRIB motif peptides and the inactive (GDP-bound) form of Cdc42.

Analysis of Transferred NOEs. Assignments of all the proton resonances of PAK2(71−92) were established using NOESY and TOCSY spectra acquired in the presence of GST−Cdc42 (Table 1). Intraresidue spin systems were identified on the basis of cross-peak patterns from the TOCSY spectra, and assigned through sequential NOE connectivities. For the three proline residues, the δCH proton was used in place of the usual NH for tracing the connectivity. The existence of NOE contacts between the αCH proton of the preceding residues and the δCH protons of Pro72, Pro76, and Pro77 indicate that all of these proline residues adopt the trans conformation in this peptide. There is, however, evidence for a slight (<10%) isomerization at Pro77, as two sets of TOCSY peaks for Ser78 were observed. Transferred NOEs corresponding to the cis form of this proline were not observed, suggesting that it is not required for interaction with Cdc42.

Figure 4 presents a schematic overview of the sequential and nonsequential NOE contacts in PAK2(71−92) induced by the binding of GTP-γS-loaded GST−Cdc42. The bulk of the observed nonsequential NOEs fall in the peptide segment between residues Pro77 and Phe88. Although no distinct patterns of defined secondary structure elements (i.e., helical or β-sheet NOE patterns) are observed, there are a series of side chain contacts between a group of aromatic and hydrophobic side chains, including the conserved Pro77, Phe80, His82, His85, and Val86. These NOE connectivities

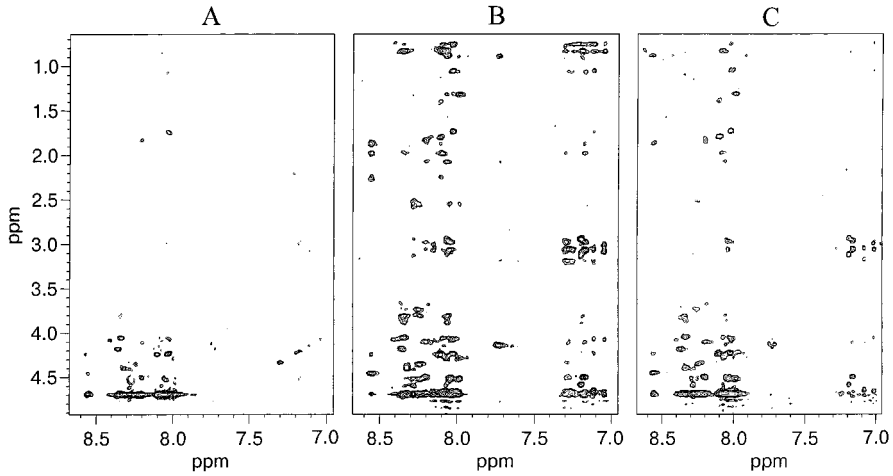

FIGURE 3: Amide and aromatic regions of the NOESY spectra of PAK2(71−92) free (A) and in the presence of GTP-γS-loaded (B) or GDP-loaded (C) Cdc42 at a 10:1 molar ratio of peptide to unlabeled GST−Cdc42. The spectra were collected at 500 MHz using a NOE mixing time of 150 ms with a sample temperature of 30 °C.

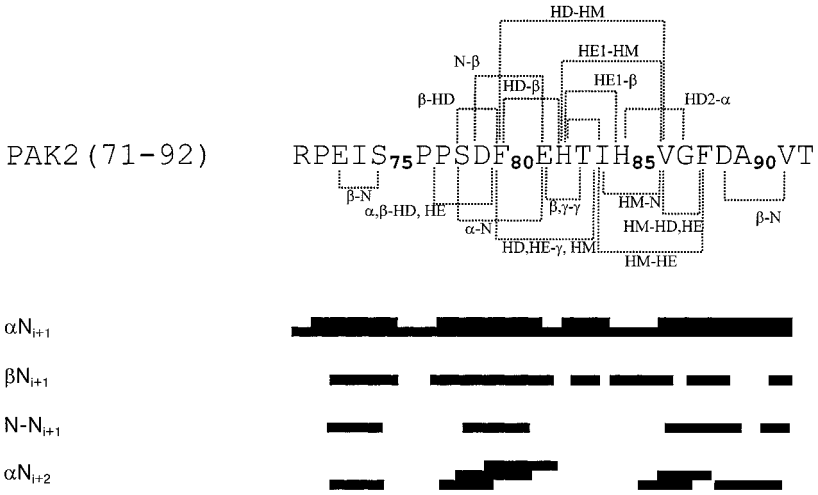

FIGURE 4: Schematic overview of the significant transferred NOEs observed for PAK2(71−92) in the presence of GST−Cdc42. Sequential and $C\alpha H_i-NH_{i+2}$ NOEs are denoted by black bars, while other NOEs are denoted by the dotted lines and labeled with the identities of the involved protons.

suggest a loop structure folded around a hydrophobic core group of residues. A series of backbone NOEs between residues Pro77 and His82, including sequential NH−NH, αN_{i+2}, and αN_{i+3} contacts, suggest a turn conformation. There are, however, no long-range NOE contacts between the C- and N-terminal regions of this peptide. The lack of nonsequential NOEs within the N-terminal region of this peptide indicates that these residues may adopt an extended conformation.

Conformation of PAK2(71−92) Bound to Cdc42. NOE intensities observed in the NOESY spectra of PAK2(71−92) in the presence of GST−Cdc42 can be converted to interproton distances representative of the bound conformation of the peptide due to a lack of significant NOE contributions either from the free peptide (Figure 3A) or from the GST−Cdc42 (*46*). Structures were calculated using a final set of 123 NOE-derived distance constraints supplemented with a limited number (~10) of conservative (3−4 Å**)** lower bound constraints. The structures derived from these calculations were superimposed well, with an average rmsd of 1.2 Å for all heavy atoms of residues between Pro77 and Ala91. The residues outside these regions are not well-defined, and the N-terminal stretch of residues, perhaps due to the lack of NOE constraints, is generally in an extended conformation. Regardless, the ensemble of calculated structures reproduced most of the observed experimental NOEs when they were subjected to NOE back calculations. A representative set of conformations was selected on the basis of a lower number of distance violations. These were superimposed using the heavy atoms of residues from Pro77 to Ala91, and are presented in Figure 5. Again, NOE constraints between residues Phe80 and His82 and a group of surrounding residues largely define the folded region of the bound peptide. The side chains of Phe80, His82, Ile84, and His85 are directed inward, toward the center of the loop, and the acidic side chains of Asp79 and Glu81 are directed outward (Figure 5).

DISCUSSION

Studies to date suggest that in the absence of Cdc42, the CRIB motif or extended Cdc42 binding sequences are not folded and even lack significant secondary structure (*20*, *21*). This lack of folding leads to difficulties in defining the minimal sequences required for binding to Cdc42. Delineating the binding region on the basis of sequence homology is also complicated as some of the potential Cdc42−Rac

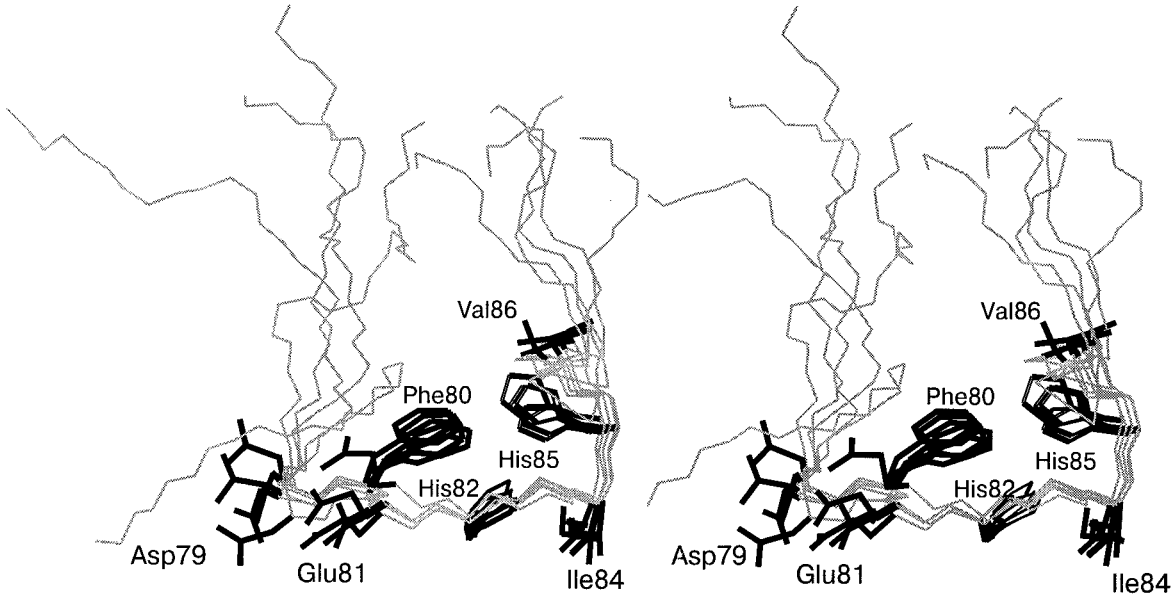

FIGURE 5: Stereodiagram of a cluster of five model structures of PAK2(71−92) from distance geometry calculations. These structures were superimposed using the backbone atoms from Pro77−Ala90. Side chains of well-defined residues are labeled, and denoted by thick lines.

ligands such as the PAK and ACK kinases (*47*) share extended regions of high homology C-terminal to the CRIB region while other candidate effectors such as WASP do not. Interestingly, interaction of PAK2(71−92) with GTP-γS-loaded Cdc42 leads to structuring of this peptide, as evidenced by the appearance of many transferred NOEs. Similar NOEs are not observed in the free peptide, and are significantly attenuated in the presence of GDP-bound Cdc42. Although the structure of the entire peptide is not well defined, residues Pro77−Ala90 fold into a unique conformation upon binding to the "active" form of Cdc42. Structure calculations revealed a loop conformation condensed around a hydrophobic cluster comprised of residues Phe80, His82, Ile84, His85, and Val86. The presence of widespread line broadening effects for this peptide in the presence of Cdc42, and the observation of numerous resonance perturbations for residues of Cdc42, point to an extended interaction surface within the complex of Cdc42 with the CRIB peptide.

The affinity of binding between Cdc42 and the CRIB peptide PAK2(71−92) was somewhat lower than that observed by other researchers (*20*, *21*, *24*) using C-terminally extended CRIB sequences based on PAK, or a 49-residue peptide used in this study derived from residues 69−117 of PAK2 (K_d value of 0.6 μM vs 30−50 nM). However, comparable fragments of WASP containing either just the CRIB motif or the CRIB motif with a 50-residue N-terminal extension exhibited affinities similar to that obtained in this study (*21*). These results suggest that the larger fragments with higher binding affinities may make further contacts with Cdc42, or perhaps stabilize a favorable conformation of the CRIB region upon interaction. This second possibility seems more likely, as interaction of PAK2(71−92) with GTP-γS-loaded Cdc42 is accompanied by changes in the environments of a large number of residues on the surface of Cdc42. A similar pattern of perturbed residues is observed compared to those recently reported by Guo et al. (*24*) for the complex of GMPPCP-loaded Cdc42 with a 46-amino acid CRIB-containing peptide based on mPAK3. Perturbations are seen both in the N-terminal third of Cdc42 and in the C-terminal helix, consistent with evidence from chimera studies that multiple sites, including both the effector domain and the C-terminal helix of Rac, are involved in the analogous Rac−CRIB interactions (*48*). These results indicate that the shorter CRIB peptide binds in the same mode as the extended protein fragments. In addition, calorimetric measurements revealed a slow heat change upon titration of another CRIB peptide PAK(75−105) with Cdc42 (*20*), suggesting conformational changes during binding, with a slightly faster transition observed for a longer fragment PAK(75−118), indicating that residues C-terminal to the CRIB motif may stabilize a favorable conformation of the CRIB region upon interaction with Cdc42.

Residues flanking the CRIB motif in some members of the PAK family of kinases also participate in negative regulation of the kinase domain. Although the PAK kinases do not appear to autophosphorylate within the CRIB region (*49*), amino acid changes either within the minimal CRIB region (H83L and H86L) (*50*) or immediately following its C-terminal region [P91S, G93A, and P95A (*3*) or L107F (*51*)] have been shown to lead to constitutive activation of these kinases. This activation may be the result of relieving a negative restraint brought about by an intermolecular interaction between the kinase domain and sequences overlapping the Cdc42 binding regions of these proteins. Indeed, a fragment of PAK [PAK(83−149)] consisting of the C-terminal region of the CRIB motif and an additional 60 residues is a potent inhibitor of PAK activation (*25*). These findings are supported by the observation that a novel member of the PAK family of protein kinases, PAK4, exhibits a reduced level of conservation in the region C-terminal to the CRIB motif compared with the other PAK-family kinases, and does not seem to be significantly activated by Cdc42 (*19*). Taken together, these studies indicate that the well-conserved sequences C-terminal to the CRIB motif are important for functions other than interaction with Cdc42.

Interactions between Cdc42 and its effectors are formally similar to those between the Ras-family GTPases and the Ras binding domain (RBD) of Ras effector kinases such as Raf. In the case of the Raf RBD, folding of an 81-residue fragment (residues 51−131) is observed in the absence of binding (*52*), with minimal structural reorganization upon interaction with the Ras homologue Rap (*53*). To date, however, no evidence for structuring of the CRIB region alone in solution has been obtained, even in extended CRIB-containing protein fragments (*20*, *21*). It is commonly assumed that potent and specific biological activity is an exclusive property of well-folded proteins or protein domains (*54*). There are, however, a growing number of reports of proteins or protein domains with key biological roles that are intrinsically unstructured under physiological conditions (*55*, *56*). Recent examples include the kinase-inducible activation domain of CREB (*57*) and the herpes simplex virus VP16 protein (*58*). These apparently unfolded proteins may express their biological functions through the formation of uniquely structured complexes with their binding partners (*56*−*58*). The observed lack of folding in CRIB-containing protein fragments, coupled with the observation that flanking sequences are in some cases involved in functions other than interaction with Cdc42, suggests that the CRIB sequence motif may not be uniquely structured in the absence of Cdc42, yet retains the ability to interact with Cdc42 with specificity and high affinity.

Most partially folded yet active proteins reported to date appear to use a subregion for their binding interactions (*57*−*59)*. This binding region can either function alone, as an autonomous domain (*59*), or promote folding of the rest of the molecule upon complexation, leading to increased binding affinity (*57*). The 22-residue peptide PAK2(71−92) characterized in this study contacts a surface on Cdc42 which approximates that of a 46-residue protein fragment previously studied, is sensitive to the nucleotide state of Cdc42, and exhibits structuring upon interaction with Cdc42. As such, this peptide may represent the minimal interfacial region responsible for the CRIB−Cdc42 interaction. In addition, the results of this study suggest that in contrast to the Raf−RBD interaction, which consists of a short stretch of interfacial β-sheet (*53*), the Cdc42−CRIB interface is more extensive, involving a larger surface area. The existence of a hydrophobic cluster in the Cdc42-bound CRIB peptide (Figure 5) implies that the peptide may also interact with a complementary crevice on Cdc42, burying the well-conserved hydrophobic residues that form the CRIB consensus. Indeed, several residues on the surface of Cdc42 that respond to peptide binding, including Ile4, Tyr51, and Ile173, form a hydrophobic cluster at the interface of strands β1−β3 and the α5 helix (*41*). These unique structural features suggest that the Cdc42-bound conformation of CRIB peptides may be a good starting point for the generation of further-minimized CRIB ligands. Determination of the three-dimensional structures of the complexes between Cdc42 and its CRIB ligands will provide further understanding of the structural details responsible for the affinity and specificity of these molecular interactions.

ACKNOWLEDGMENT

We thank Drs. David Thomas, Malcolm Whiteway, Cunle Wu, Andre Nantel, and Ekkehard Leberer for helpful discussions. We also thank Andy Ng and Zhigang Chen for carrying out preliminary work with human Cdc42 and Pak2 peptides, respectively, and Betty Zhu for help with the structural calculations.

REFERENCES

1. Symons, M. (1996) *Trends Biol. Sci. 21*, 178−181.
2. Chou, M. M., and Blenis, J. (1996) *Cell 85*, 573−583.
3. Bagrodia, S., Dérijard, B., Davis, R. J., and Cerione, R. A. (1995) *J. Biol. Chem. 270*, 27995−27998.
4. Zigmond, S. H. (1996) *Curr. Opin. Cell. Biol. 8*, 66−73.
5. Ridley, A. J. (1996) *Curr. Biol. 6*, 1256−1264.
6. Allen, K. M., Gleeson, J. G., Bagrodia, S., Partington, M. W., MacMillan, J. C., Cerione, R. A., Mulley, J. C., and Walsh, C. A. (1998) *Nat. Genet. 20*, 25−30.
7. Chuang, T.-H., Hahn, K. M., Lee, J.-D., Danely, D. E., and Bokoch, G. M. (1997) *Mol. Biol. Cell 8*, 1687−1698.
8. Keely, P. J., Westwick, J. W., Whitehead, I. P., Channing, J. D., and Parise, L. V. (1997) *Nature 390*, 632−636.
9. Burbelo, P. D., Dreschel, D., and Hall, A. (1995) *J. Biol. Chem. 270*, 29071−29074.
10. Sells, M. A., and Chernoff, J. (1997) *Trends Cell. Biol. 7*, 162−167.
11. Manser, E., Leung, T., Salihuddin, H., Tan, L., and Lim, L. (1993) *Nature 363*, 364−367.
12. Yang, W., and Cerione, R. A. (1997) *J. Biol. Chem. 272*, 24819−24824.
13. Leung, T., Chen, X.-Q., Tan, I., Manser, E., and Lim, L. (1998) *Mol. Cell. Biol. 18*, 130−140.
14. Aspenström, P., Lindberg, U., and Hall, A. (1996) *Curr. Biol. 6*, 70−75.
15. McCallum, S. J., Wu, W. J., and Cerione, R. A. (1996) *J. Biol. Chem. 271*, 21732−21737.
16. Manser, E., Leung, T., Salihuddin, H., Zhao, Z., and Lim, L. (1994) *Nature 367*, 40−46.
17. Symons, M., Derry, J. M. J., Larlak, B., Jiang, S., Lemahieu, V., McCormick, F., Franke, U., and Abo, A. (1996) *Cell 84*, 723−734.
18. Leberer, E., Wu, C., Leeuw, T., Fourest-Lieuvin, A., Segall, J. E., and Thomas, D. Y. (1997) *EMBO J. 16*, 83−97.
19. Abo, A., Qu, J., Cammarano, M. S., Dan, C., Fritch, A., Baud, V., Belisle, B., and Minden, A. (1998) *EMBO J. 22*, 6527−6540.
20. Thompson, G., Owen, D., Chalk, P. A., and Lowe, P. E. (1998) *Biochemistry 37*, 7885−7891.
21. Zhang, B., Wang, Z.-X., and Zheng, Y. (1997) *J. Biol. Chem. 272*, 21999−22007.
22. Leonard, D. A., Satoskar, R. S., Wu, W., Bagrodia, S., Cerione, R. A., and Manor, D. (1997) *Biochemistry 36*, 1173−1180.
23. Rudolph, M. G., Bayer, P., Abo, A., Kuhlmann, J. M., Vetter, I., and Wittinghofer, A. (1998) *J. Biol. Chem. 273*, 18067−18076.
24. Guo, W., Sutcliffe, M. J., Cerione, R. A., and Oswald, R. E. (1998) *Biochemistry 37*, 14030−14037.
25. Zhao, Z.-S., Manser, E., Chen, X.-Q., Chong, C., Leung, T., and Lim, L. (1998) *Mol. Cell. Biol. 18*, 2153−2163.
26. Leonard, D. A., Evans, T., Hart, M., Cerione, R. A., and Manor, D. (1994) *Biochemistry 33*, 12323−12328.
27. Nomanbhoy, T. K., Leonard, D. A., Manor, D., and Cerione, R. A. (1996) *Biochemistry 35*, 4602−4608.
28. Jeener, J., Meier, B. H., Bachmann, P., and Ernst, R. R. (1979) *J. Chem. Phys. 71*, 4546−4553.
29. Braunschweiler, L., and Ernst, R. R. (1983) *J. Magn. Reson. 53*, 521−528.
30. Davis, D. G., and Bax, A. (1985) *J. Am. Chem. Soc. 107*, 2820−2821.
31. Mori, S., Abeygunawardana, C., Johnson, M. O., and VanZijl, P. C. M. (1995) *J. Magn. Reson., Ser. B 108*, 94−98.
32. Kay, L. E., Ikura, M., Tschudin, R., and Bax, A. (1990) *J. Magn. Reson. 89*, 496−514.
33. Grzesiek, S., and Bax, A. (1992) *J. Magn. Reson. 89*, 496−514.
34. Bax, A., and Ikura, M. (1991) *J. Biomol. NMR 1*, 99−104.

35. Piotto, M., Saudek, V., and Sklenar, V. (1992) *J. Biomol. NMR 2*, 661.
36. Sklenar, V., Piotto, M., Leppik, R., and Saudek, V. (1993) *J. Magn. Reson., Ser. A 102*, 241.
37. Talluri, S., and Wagner, G. (1996) *J. Magn. Reson., Ser. B 112*, 200−205.
38. Mueller, L., and McCoy, M. A. (1992) *J. Am. Chem. Soc. 114*, 2108.
39. Delaglio, F., Grzesiek, S., Vuister, G. W., Zhu, G., Pfiefer, J., and Bax, A. (1993) *J. Biomol. NMR 6*, 277−293.
40. Bartels, C., Xia, T.-H., Billeter, M., Guntert, P., and Wutrich, K. (1995) *J. Biomol. NMR 6*, 1−10.
41. Feltham, J. L., Dotsch, V., Raza, S., Manor, D., Cerione, R., Sutcliffe, M. J., Wagner, G., and Oswald, R. E. (1997) *Biochemistry 36*, 8755−8766.
42. Ni, F., and Zhu, Y. (1994) *J. Magn. Reson., Ser. B 102*, 180−184.
43. Ning, Q., Ripoll, D. R., Szewczuk, Z., Konishi, Y., and Ni, F. (1994) *Biopolymers 4*, 1125−1137.
44. Némethy, G., Gibson, K. D., Palmer, K. A., Yoon, C. N., Paterlini, G., Zagari, A., Rumsey, S., and Scheraga, H. A. (1992) *J. Phys. Chem. 96*, 6472−6484.
45. Vasquez, M., and Scheraga, H. A. (1988) *J. Biomol. Struct. Dyn. 5*, 757−784.
46. Ni, F. (1994) *Prog. NMR Spectrosc. 26*, 517−606.
47. Manser, E., Leung, T., Salihuddin, H., Zhao, Z., and Lim, L. (1994) *Nature 367*, 40−46.
48. Diekmann, D., Nobes, C. D., Burbelo, P. D., Abo, A., and Hall, A. (1995) *EMBO J. 14*, 5297−5305.
49. Manser, E., Huang, H.-Y., Loo, T.-H., Chen, X.-Q., Dong, J.-M., Leung, T., and Lim, L. (1997) *Mol. Cell. Biol. 17*, 1129−1143.
50. Tang, Y., Chen, Z., Ambrose, D., Liu, J., Gibbs, J. B., Chernoff, J., and Field, J. (1997) *Mol. Cell. Biol. 17*, 4454−4464.
51. Brown, J. L., Stowers, L., Baer, M., Trejo, J., Coughlin, S., and Chant, J. (1996) *Curr. Biol. 6*, 598−605.
52. Emerson, S. D., Waugh, D. S., Scheffler, J. E., Tsao, K. L., Prinzo, K. M., and Fry, D. C. (1994) *Biochemistry 33*, 7745−7752.
53. Nassar, N., Horn, G., Herrmann, L., Scherer, A., McCormic, F., and Wittinghoefer, A. (1995) *Nature 375*, 554−560.
54. Anfinsen, C. B. (1973) *Science 181*, 223−230.
55. Plaxco, K. W., and Gross, M. (1997) *Nature 386*, 657−659.
56. Dyson, H. J., and Wright, P. E. (1998) *Nat. Struct. Biol.* (NMR Suppl.), 499−503.
57. Radhakrishnan, I., Perez-Alvarado, G. C., Parker, D., Dyson, H. J., Montminy, M. R., and Wright, P. E. (1997) *Cell 91*, 741−752.
58. Uesugi, M., Nyanguile, O., Lu, H., Levine, A. J., and Verdine, G. A. (1998) *Science 277*, 1310−1313.
59. Fletcher, C. M., McGuire, A. M., Gingras, A.-C., Li, H., Matsuo, H., Sonenberg, N., and Wagner, G. (1998) *Biochemistry 37*, 9−15.

BI990426U